

Two-step contributions in the $^{206}\text{Pb}(\vec{t},p)^{208}\text{Pb}$ two-neutron transfer reaction

W. P. Alford

The University of Western Ontario, London, Ontario, Canada N6A 3K7

R. N. Boyd

The Ohio State University, Columbus, Ohio 43210

E. Sugarbaker* and F. W. N. de Boer†

University of Colorado, Boulder, Colorado 80302

Ronald E. Brown and E. R. Flynn

Los Alamos National Laboratory, Los Alamos, New Mexico 87545

(Received 28 October 1981)

The $^{206}\text{Pb}(\vec{t},p)$ reaction has been studied over the angular range from 10° to 60° at a triton energy of 17 MeV. Cross sections and analyzing powers were measured for 11 states between 2.6 and 5.0 MeV excitation, including the 4^- state at 3.475 MeV. The two-neutron transfer reaction to this state was represented by a sequential transfer calculation. Data for three natural parity states, in particular the analyzing powers, were not fitted well by one-step distorted-wave Born approximation calculations. Numerous sequential transfer calculations with different transfer configurations were tried for each of these states. While most of the calculations produced results similar to the distorted-wave Born approximation results, at least one calculation was found for each state which gave an improved representation over that of the distorted-wave Born approximation. The failure of the distorted-wave Born approximation documents the need to apply sequential transfer reaction processes in general descriptions of two-nucleon transfer reactions.

[NUCLEAR REACTIONS: $^{206}\text{Pb}(\vec{t},p)^{208}\text{Pb}$, $E = 17$ MeV; measured $\sigma(\theta)$, $A_y(\theta)$. DWBA and sequential transfer calculations.]

INTRODUCTION

The study of two-nucleon transfer reactions such as (t,p) has provided a wealth of nuclear structure information. Most experimental results have been analyzed using the standard DWBA theory, which assumes the simultaneous transfer of a zero-coupled pair between the target and the incident projectile. In the normal zero-range approximation this theory is moderately successful in fitting the shapes of cross-section angular distributions to strongly excited states, but it is often unable to reproduce details of the data without significant parameter adjustment.¹ Furthermore, some two-nucleon transfers cannot be represented at all by this scheme. For example, transitions from spin-zero targets to states of unnatural parity are predicted to be completely forbidden.

Attempts to remove some of the known

shortcomings of the usual theory have led to the introduction of finite-range calculations,^{2,3} to the use of more complex wave functions for the triton internal structure,^{2,4} and to two-step mechanisms, often including several reaction channels, for the transfer of the two nucleons.^{5,6} There is no question that calculations should in principle use finite-range interactions and a realistic triton wave function. The resultant computations are much more difficult than zero-range calculations, however, and several studies have shown that for allowed transitions the predicted angular distributions show little change in shape when compared with results of the standard theory.³ On the other hand, calculations assuming two-step, inelastic excitations have been able to account for measured angular distributions for strong allowed transitions which were in serious disagreement with DWBA predictions.⁷ Two-step calculations assuming sequential transfer of the two nucleons have also

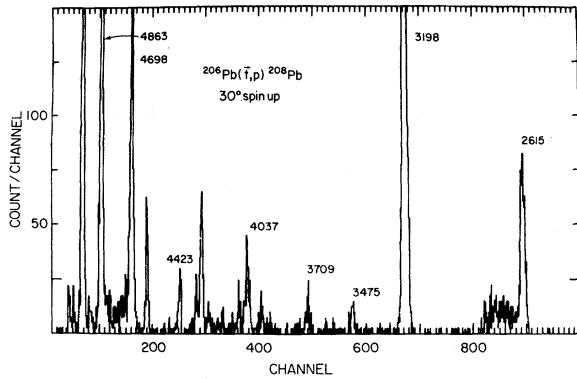


FIG. 1. Proton spectra from the $^{206}\text{Pb}(\vec{t},p)^{208}\text{Pb}$ reaction. Selected peaks are labeled with their excitation energy in keV.

been able to account for unnatural parity transitions in several nuclei including ^{16}O ,⁸ ^{20}Ne ,⁹⁻¹¹ ^{28}Si ,¹² ^{58}Fe ,¹³ $^{58,60}\text{Ni}$,^{13,14} and ^{206}Pb .^{6,12,15,16} The last case is particularly interesting because of the simple structure of the 3^+ (1.34 MeV) final state in ^{206}Pb . Another study⁴ has shown, however, that this transition can be accounted for if finite-range effects and a realistic triton wave function are used in a one-step calculation and has suggested that it is not necessary to consider the sequential transfer mechanism. More recently though, measurements of the asymmetry A_y for ground-state transitions in (\vec{p},t) reactions have led to the conclusion that sequential transfer can be an important mechanism, even in strong allowed transitions.^{17,18}

Thus the present measurements were undertaken to study two-neutron transitions to ^{208}Pb states having fairly well known wave functions in the hope that measurements of both cross section and analyzing power would provide a clear indication of the reaction mechanism involved. Particular attention has been focused on the ^{208}Pb (4^- , 3.475 MeV) state, since the possible reaction mechanisms populating it are more restricted than for the natural parity states.

EXPERIMENTAL

Measurements were carried out using the polarized triton beam¹⁹ from the Los Alamos tandem Van de Graaff facility. The beam energy was 17 MeV and beam currents were typically about 50 nA with a beam polarization of about 0.75, determined from measurements of the quench ratio.²⁰ The target consisted of metallic lead enriched to 99.7% in ^{206}Pb , evaporated on a thin carbon backing. The target thickness was measured by elastic scattering to be 1.1 mg/cm^2 . Reaction protons were recorded using a helical delay line counter²¹ in the focal plane

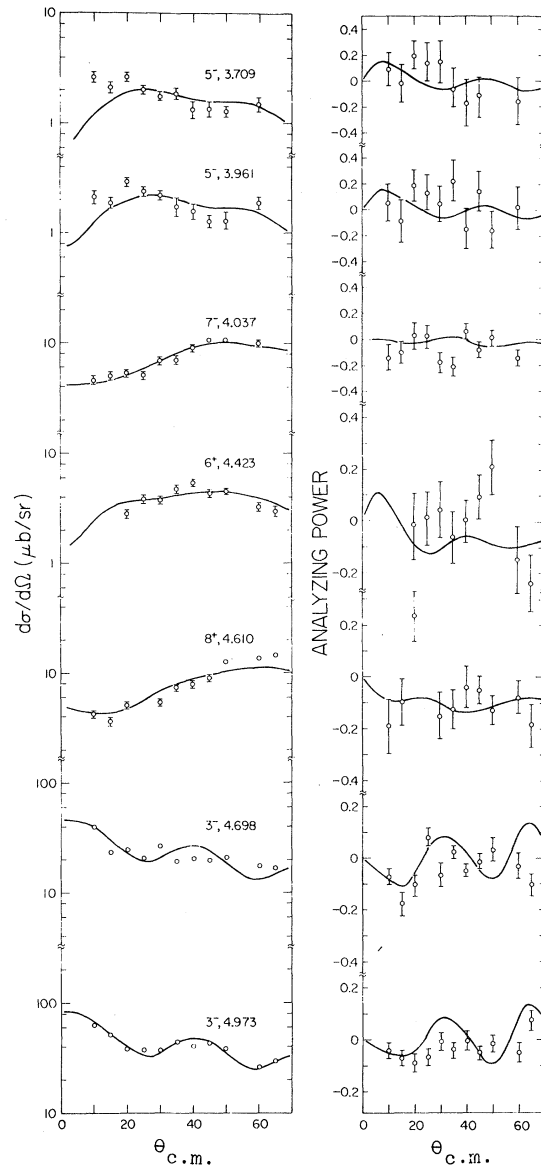


FIG. 2. Angular distributions of cross section and analyzing power for transitions fitted with one-step DWBA calculations.

of the Q3D magnetic spectrograph. At each angle, measurements of beam polarization and reaction yield for each polarization state were carried out in a computer-controlled sequence with experimental parameters and spectra recorded on magnetic tape. The overall energy resolution in the measurements was about 25 keV. Measurements were carried out at intervals of 5° between the angles of 10° and 60° .

RESULTS

A typical spectrum is shown in Fig. 1. The energy calibration for this spectrum was obtained from the

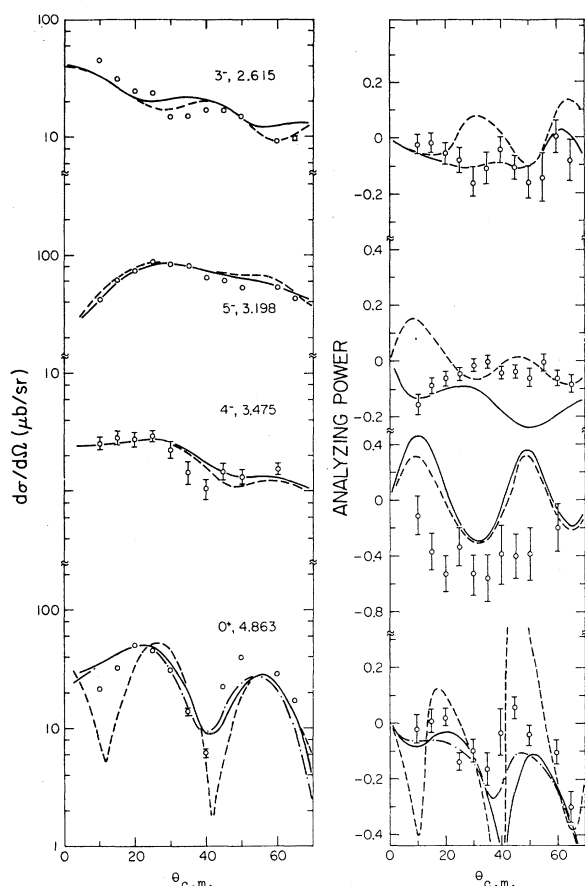


FIG. 3. Angular distributions of cross section and analyzing power for transitions fitted with two-step calculations. The significance of the calculated curves is discussed in the text.

known energies of the clearly resolved groups labeled in the figure. All groups observed in the spectrum could be correlated with known levels in ^{208}Pb , but no analysis was carried out for the region between the levels at 4037 and 4423 keV excitation, because of low cross sections for most groups in this region, along with problems from contaminant groups.

Measured angular distributions of differential cross section and analyzing power are shown in Figs. 2 and 3. The curves are the results of calcula-

tions discussed below. Error bars on the data points reflect statistical uncertainties only. For the weaker transitions shown in Fig. 2, uncertainties in the analyzing power are large, and the comparison with the DWBA predictions does not provide a very significant model comparison. However, the data for the 3^- states at 4.698 and 4.973 MeV may be in disagreement with the DWBA predictions.

$^{206}\text{Pb}(t,p)$ reaction calculations

Reaction calculations were performed from two quite different viewpoints. Firstly, the reaction was assumed to proceed, at least for the natural parity transitions, via the conventional one-step transfer of a spin-zero coupled neutron pair. All calculations assumed zero-range interactions and local potentials. An examination of the present results confirms some of the above mentioned difficulties with the normal DWBA description of two-neutron transfer. That description produces both differential cross sections and analyzing powers with shapes which depend only on the angular momentum transfer, and which therefore are independent of nuclear structure. In this experiment two strongly populated 5^- states, the 3.198 and 3.709 MeV states, were observed to have very similarly shaped differential cross sections, but dramatically different forward-angle analyzing powers. Because the conventional one-step reaction description produces angular distributions which depend only on the L transfer, it must fail to describe the reaction to at least one of these two states. Other difficulties with the one-step transfer predictions are noted below.

Thus we have, in the present analysis, also performed sequential transfer (t,d,p) calculations for several of the ^{208}Pb states observed. States selected for this analysis were those which had sufficiently good statistics for the data or a sufficiently prominent feature in one of the angular distributions (differential cross section or analyzing power) which was not represented by the results of the one-step calculation to warrant a detailed investigation. The data for the states for which only the one-step calculations were performed are shown, together with the results of those calculations, in Fig. 2. Those data

TABLE I. Optical model parameters used in analysis. Well depths are in MeV, lengths in Fermis. The Coulomb radius parameter was $r_C = 1.3 F$ in each case.

	V_0	r_0	a_0	W_v	W_D	r_w	a_w	V_{so}	r_{so}	a_{so}
t	165.5	1.16	0.769	13.9		1.442	0.864	6.0	1.15	0.73
d	106.2	1.10	0.82		7.56	1.51	0.82	6.8	1.07	0.66
p	58.5	1.17	0.75	1.5	9.6	1.32	0.658	6.2	1.01	0.75

for states for which both types of calculations were performed, or for which the two-step calculation was required (the 4^- state), are shown in Fig. 3. Each type of calculation is described in detail below.

The one-step calculations used the coupled channel Born approximation (CCBA) code CHUCK,²² which was run in the DWBA mode for these calculations. The form factor utilized the Bayman-Kallio prescription²³ for two-nucleon transfer, and a variety of possible shell-model configurations were tried. These were guided by the ^{206}Pb wave functions of True,²⁴ and the ^{208}Pb wave functions of True *et al.*,²⁵ but were not restricted to the transfers predicted by those wave functions. In several cases a number of different transfer configurations were tried. The result is, as noted above, that the specific shell-model configurations have virtually no effect on the shape of the differential cross section or on the shape or magnitude of the analyzing power. The only feature which is affected by the specific orbits of the transferred particles in the one-step reaction

description is the magnitude of the predicted cross section.

The optical parameters used in the calculations are shown in Table I. The one-step calculation utilized the triton parameters of Flynn *et al.*²⁶ with a spin-orbit term taken to be the average strength and geometry obtained in the survey study of Hardekopf *et al.*,²⁷ and the proton parameters of Becchetti and Greenlees²⁸ ($r_0=1.17$ fm set). The bound-state well was taken to have a geometry of $(r_0, a)=(1.17, 0.75)$, and the binding energy of each of the two neutrons was taken to be half the two-neutron binding energy for the state being considered. The recommended value of the zero-range factor²² of $1560 \text{ MeV}^{1/2} \text{ fm}^{3/2}$ was used in the calculations. (That factor also includes a normalizing factor of $\sqrt{9.7}$ to give the proper normalization for the two-nucleon transfer form factor as it is programmed in CHUCK.²²)

The data comparisons for the states which were represented reasonably well by the one-step calculations are shown in Fig. 2. In Table II are listed the

TABLE II. Details of reaction calculations for $^{206}\text{Pb}(\vec{t},p)^{208}\text{Pb}$.

^{208}Pb state, ex. energy	Type of calculation	Transfer configuration	Scaling factor ^a	Fit to $d\sigma/d\Omega(\theta)$	Fit to $A(\theta)$	Dominant theoretical configuration ^b	Shown in figure
3 ⁻ , 2.615	DWBA	$g_{9/2}f_{5/2}$	6.3	fair	poor	mixed	3, dashed
	CRC	$p_{1/2}g_{7/2}$	0.33	fair	good		3, solid
5 ⁻ , 3.198	DWBA	$g_{9/2}p_{1/2}$	1.67	good	poor	$p_{1/2}g_{9/2}$	3, dashed
		$p_{1/2}i_{11/2}$	20.0	good	poor		3, dashed
	CRC	$p_{1/2}i_{11/2}$	6.0	good	fair		not shown
		$\sqrt{0.1}p_{3/2}g_{7/2} +$ $\sqrt{0.9}p_{1/2}i_{11/2}$	2.0	good	fair		3, solid
4 ⁻ , 3.475	CRC	$p_{1/2}g_{9/2}$	0.25	good	fair	$p_{1/2}g_{9/2}$	3, solid
		$\sqrt{0.7}p_{1/2}g_{9/2} +$ $\sqrt{0.3}f_{5/2}g_{9/2}$	0.67	good	fair		3, dashed
	DWBA	$f_{5/2}g_{9/2}$	0.22	fair	good	$f_{5/2}g_{9/2}$ or $p_{1/2}g_{9/2}$	2
5 ⁻ , 3.709	DWBA	$f_{5/2}g_{9/2}$	0.18	fair	good	$f_{5/2}g_{9/2}$	2
5 ⁻ , 3.961	DWBA	$p_{1/2}i_{11/2}$	0.42	fair	good		2
	DWBA	$f_{5/2}g_{9/2}$	0.34	good	fair	$f_{5/2}g_{9/2}$	2
7 ⁻ , 4.037	DWBA	$p_{3/2}j_{15/2}$	0.50	good	fair		2
8 ⁺ , 4.610	DWBA	$p_{1/2}j_{15/2}$	1.94	good	good		2
3 ⁻ , 4.698	DWBA	$p_{3/2}g_{9/2}$	0.36	fair	fair	$f_{5/2}g_{9/2}$ or $p_{3/2}g_{9/2}$	2
0 ⁺ , 4.863	DWBA	$g_{9/2}^2$	5.5	poor	poor	mixed	3, dashed
	CRC	$g_{9/2}^2$	2.5	fair	poor		3, solid
		$\sqrt{0.82}g_{9/2}^2 -$ $\sqrt{0.09}s_{1/2}^2 -$ $\sqrt{0.09}p_{1/2}^2$	1.1	fair	fair		3, dotted-dashed
	DWBA	$p_{1/2}d_{5/2}$	0.48	good	fair	mixed	2

^aDefined as $(d\sigma/d\Omega)_{\text{exp}}/(d\sigma/d\Omega)_{\text{theor}}$.

^bInferred from Refs. 24 and 25.

states for which those calculations were performed, the configurations assumed for the transferred nucleons, and the factor by which the calculated cross section had to be multiplied to produce the fit to the data shown in Fig. 2. Only the 8^+ , 4.610 MeV level has an observed cross section which is larger than that given by a single transfer configuration calculation. Even in that case the predicted cross section is close enough to that observed that some admixed transfer configurations could readily produce a cross section of the observed magnitude.

The sequential transfer coupled reaction channel (CRC) calculations were also performed with the code CHUCK.²² The triton and proton parameters used were the same as for the one-step calculations, while the deuteron parameters for intermediate states were those of Childs *et al.*²⁹ with a spin-orbit term taken from Daehnick *et al.*³⁰ For most of the calculations it was assumed that only the states characterized by ^{207}Pb (J^π) and a triplet deuteron contributed, but a few calculations were tried to determine the possible influence of the deuteron singlet state. The Q values and binding energies for the intermediate channels were those associated with the discrete states in ^{207}Pb (primarily the $\frac{1}{2}^-$, g.s.; $\frac{5}{2}^-$, 0.570 MeV; $\frac{9}{2}^+$, 2.728 MeV; and $\frac{11}{2}^+$, 3.509 MeV states). These states were assumed to have sufficient neutron stripping strength in $^{206}\text{Pb}(t,d)$ to serve as intermediate states in the two neutron transfer; this assumption has been observed³¹ to be approximately valid for all of the results discussed below. The recommended zero-range factors of $D_0 = 183(123) \text{ MeV}^{1/2} \text{ fm}^{3/2}$ were used for the (t,d) ((d,p)) transfers.

The most critical test of the assumed (t,d,p) reaction mechanism is provided by the ^{208}Pb (4^- , 3.475 MeV) state, since it must be populated by some mechanism other than the usual one-step process. Since most possibilities other than sequential transfer would appear to have been precluded,¹ the (t,d,p) process was assumed to be the dominant one. The wave functions²³ for 4^- states in ^{208}Pb suggest that the two neutrons should be transferred mainly into a $p_{1/2}$ and a $g_{9/2}$ orbit, but that a $f_{5/2}g_{9/2}$ transfer configuration could also contribute significantly. The results of the calculation assuming only the $p_{1/2}g_{9/2}$ transfer configuration are shown as the solid curves in conjunction with the data for the 4^- level in Fig. 3; the representation of the cross section is fairly good, but the predicted analyzing power is shifted upward from the data. The results of another calculation, in which the transfer configuration was assumed to be

are illustrated by the dashed curves in Fig. 3 and show the effects of small admixed configurations. Additional admixed configurations, e.g., $p_{3/2}g_{9/2}$, would be expected to improve the data representation further (with the phase chosen appropriately).

It should be noted that the calculations for this state exhibited a large sensitivity to the optical-model parameters used, particularly those for the deuteron channel. Use of the global deuteron potential set of Daehnick *et al.*³⁰ produced a cross section minimum at 28° , well out of phase with the observed cross section. Because of this parameter sensitivity, further tuning of the transfer configuration to achieve better fits to the data for this state was not deemed meaningful.

The ^{208}Pb (3^- , 2.615 MeV), and ^{208}Pb (5^- , 3.198 MeV) states both have differential cross sections which are fairly well represented by the results of one-step calculations (the dashed curves in Fig. 3). In both cases, however, the analyzing powers are poorly represented by the one-step results. For the 3^- state, the predicted analyzing power in the region between 15° and 30° is badly out of phase with the data. The forward-angle analyzing power representation of the one-step result is quite poor for the 5^- state.

Thus CRC calculations were also performed for those states. Most details of the calculations are the same as those described above for the 4^- state, but with neutron binding energies and Q values adjusted to the appropriate values. The 3^- state is thought²³ to be highly collective, with a very complex wave function. Since it was not possible to carry out sequential transfer calculations for this state with a realistic form factor, calculations were carried out (not shown in Fig. 3) assuming transfer configurations of $p_{3/2}g_{9/2}$, $f_{5/2}g_{9/2}$, and $p_{3/2}g_{7/2}$. These produced results very similar to the one-step predictions shown by the dashed curves. Slight changes in the predicted analyzing powers were observed for the different configurations, but no change was seen in the general features. The solid curves, in conjunction with the data for the 3^- level, show the results of a calculation assuming a $p_{1/2}g_{7/2}$ transfer configuration. They are qualitatively different from the other curves, particularly in the predicted analyzing powers around the 30° region. Those predictions achieve a rather remarkable representation of the data for the 3^- state. The results of the calculations for this state are summarized in Table II.

Since the 3^- state in the ^{208}Pb is highly collective, a coupled channels calculation was carried out assuming $L=0$ two-neutron transfer and $L=3$ inelastic excitation, with both possible orders included. The predicted cross section is much smaller than the one-step result, and it is concluded that this reaction

$$\sqrt{0.7}p_{1/2}g_{9/2} + \sqrt{0.3}f_{5/2}g_{9/2},$$

mode is probably unimportant for the present study.

The analysis for the data for the 5^- , 3.198 MeV state was similar to that for the 3^- , 2.615 MeV state. The CRC calculation (not shown in Fig. 3) assuming a $p_{1/2}g_{9/2}$ configuration, which is the dominant configuration predicted by shell model calculations,^{24,25} produced an analyzing power and cross section nearly identical to that resulting from the one-step calculation. However, it was found that two CRC calculations, namely those assuming $p_{1/2}i_{11/2}$ and $p_{3/2}g_{7/2}$ transfer configurations, do produce results which are quite different from all the one-step results, and from the other two-step results as well. Results of the calculations using a mixture (Table II) of those configurations are seen, by the solid curves in Fig. 3, to greatly improve the fit to the forward-angle analyzing-power data. Presumably mixing of other configurations and tuning of the relative amounts of those transfer configurations would improve the data representation further. Note also (Table II) that the predicted sequential transfer cross section is a factor of 3 larger than the one-step cross section, as is indicated by the two $p_{1/2}i_{11/2}$ transfer results.

The results of a one-step calculation to the ^{208}Pb (0^+ 4.863 MeV) level exhibit a problem typical of $L=0$ two-nucleon transfer results, namely, the sharp features of the theoretical results lag those of the data by several degrees for reactions at the incident energies used in this experiment. This is shown by the dashed curve in Fig. 3. Furthermore, the shapes of the angular distributions are nearly independent of the configuration assumed.

Shell-model wave functions for this state have been published,^{24,32} but are too complex to permit their use in CRC calculations. In order to obtain some estimate of the effect of the assumed transfer configurations, several CRC calculations were tried assuming a variety of transfer configurations. Those with $g_{9/2}^2$ transfer produced the results shown as the solid curves in Fig. 3. They represent the data much better than do the one-step results (and yield about twice as large a cross section), but still have the same phase around 40° as do the one-step results. Addition of a small $s_{1/2}^2$ transfer configuration, however, shifts the features of the angular distributions to the left, but still gives much too large an analyzing power near the 40° interference minimum. Several transfer configurations in the CRC calculations, e.g., $p_{1/2}^2$ and $f_{5/2}^2$, produced a cross section which peaks around 40° , thus moderating the analyzing power. The transfer configuration used to produce the dotted-dashed curves shown with the data for the 0^+ level in Fig. 3 was

$$\sqrt{0.82}g_{9/2}^2 - \sqrt{0.09}s_{1/2}^2 - \sqrt{0.09}p_{1/2}^2.$$

These curves are seen to produce quite an acceptable data representation, particularly of the phase of the angular distributions. However, it should be noted that other configurations probably could do about as well.

CRC calculations were also performed to the 4^- , 3.475 MeV and 5^- , 3.198 MeV states, using the same intermediate states in ^{207}Pb as before, but assuming that the intermediate state deuteron was in a singlet rather than a triplet state. It was found that the resulting shapes of the angular distributions are nearly identical to those produced by assuming the triplet deuteron, but the magnitudes of the cross sections are different. Using the same zero-range scaling factor (there is considerable uncertainty as to what that value should be for the singlet calculation) as was used for the triplet-deuteron calculations, the singlet cross section is, in one case, 2.5 times as large as the triplet cross section. But in the other case, the singlet cross section is 0.33 times as large as the triplet cross section. Thus no general statement can be made about the significance of the intermediate singlet deuteron states; they may be important in some cases.

It should be noted that in this study reaction calculations were carried out assuming either a one-step or a two-step reaction mechanism. It might be expected^{16,17} that both one- and two-step contributions would be involved in allowed transitions. In the absence of theoretical guidance as to the double counting which can arise from mixing the two mechanisms, it was decided to adopt the approach of the current work, namely, to assume *either* a one- or a two-step mechanism.

DISCUSSION

This reaction analysis focused on differences in shapes between predicted and observed differential cross sections, and on differences in the predicted and observed analyzing powers, to draw conclusions about the need for complex reaction processes in the theoretical description of two-nucleon transfer. Our calculations ignored both the effects of finite range and of the triton wave function. The inclusion of finite range, however, has been shown to affect primarily the magnitude of the differential cross section, so would not be expected to have much effect on our conclusions. This emphasis on theoretical-experimental differences in shapes to infer reaction mechanism information allowed conclusions which are independent of nuclear structure. All transfer configurations coupling to the same L transfer produce the same shapes of both differential cross sections and of analyzing powers in the traditional one-step prescription of two-nucleon transfer. This

observation of itself documents the inadequacy of that reaction description, since the current study has produced two pairs of states populated by the same (natural parity) L transfer which have markedly different analyzing powers.

The importance of finite-range effects for forbidden transitions is still an open question at this point. A good fit to a differential cross section using finite-range, single-step calculations was reported by Nagarajan *et al.*⁴ Another study for the same transition reported that finite-range effects are much less important than the sequential transfer effects.³³ The latter study used full finite range with spin-orbit potentials, and deuteron D -state effects were taken into account. However, the calculation only gave a qualitative representation of the analyzing power data, and the inclusion of the finite-range calculation had almost no effect on that distribution. Thus this result supports the conclusions of the present work, namely, that the second order processes are the *only* mechanisms which have yet been demonstrated to be capable of producing the differences in analyzing powers, seen in the present study, for transfer to states of the same J^π .

In the present work, features of the data were used to infer information about wave functions of the states involved. This approach was necessitated by the inability, in some cases, of the configuration predicted from shell-model calculations to be the dominant one to give a representation of the data in either a one- or two-step calculation. This does not imply that the shell model results are grossly in error, but rather that one or more of the factors indicated below is significant. Firstly, in some cases a small piece of the wave function produced an enhanced contribution to the (t,p) reaction, thereby reducing the importance of the dominant piece of the wave function. Secondly, a correct reaction description may require either more reaction trajectories than were included in the present analysis, or

the inclusion of interference effects between one- and two-step amplitudes.

This approach to analysis of the data could not have been utilized in past analyses, primarily because virtually all such analyses have been performed with one-step calculations, which produce angular distribution shapes independent of nuclear structure. The fact that distinct features, primarily in the analyzing powers, are observed, and that these features can be reproduced with CRC calculations, suggests that structure information can be gleaned from such analyses. It should also be noted that in cases in which the cross sections predicted in one- and two-step calculations were compared, the predicted magnitudes were appreciably larger for the two-step cases.

Thus two major points emerge from the current work. Firstly, the sequential transfer process in two-nucleon transfer must be included for a correct reaction description; indeed it appears often to be the *dominant* reaction mode. Secondly, the use of analyzing power data in two-nucleon transfer reaction analyses is critical. The need to represent these data in addition to the cross section data provides the possibility not only of determining the reaction mechanism involved, but also of decoupling the questions of reaction mechanism and structure.

ACKNOWLEDGMENTS

We would like to thank R. A. Hardekopf and the operating crew of the Los Alamos Van de Graaff facility for their efforts in providing the polarized triton beam. We are also indebted to S. Orbesen for maintaining the spectrograph and the helix counter, and to J. Gurskey for making the target. This work was supported by the Canadian NSERV, the U.S. National Science Foundation, and the U.S. Department of Energy.

*Present address: Physics Department, Ohio State University, Columbus, OH 43210.

†Present address: University of Fribourg, c/o SIN, 5234 Villigen, Switzerland.

¹R. N. Boyd, in *Polarization Phenomena in Nuclear Physics—1980 (Fifth International Symposium, Santa Fe)*, Proceedings of the Fifth International Symposium on Polarization Phenomena in Nuclear Physics, AIP Conf. Proc. No. 69, edited by G. G. Ohlsen, R. E. Brown, N. Jarmie, M. W. McNaughton, and G. M. Hale (AIP, New York, 1981), p. 373.

²M. F. Werby, M. R. Strayer, and M. A. Nagarajan, *Phys. Rev. C* **21**, 2235 (1980).

³B. F. Bayman and D. H. Feng, *Nucl. Phys.* **A205**, 513, (1973); L. A. Charlton, *Phys. Rev. C* **12**, 351 (1975).

⁴M. A. Nagarajan, M. R. Strayer, and M. F. Werby, *Phys. Lett.* **68B**, 421 (1977).

⁵N. B. de Takacsy, *Phys. Rev. Lett.* **31**, 1007 (1973); K. Yagi, S. Kunori, Y. Aoki, Y. Higashi, J. Sanada, and V. Tagishi, *ibid.* **40**, 161 (1978).

⁶V. Managoli and D. Robson, *Nucl. Phys.* **A252**, 354 (1974).

⁷R. J. Ascuitto, N. K. Glendenning, and B. Sorensen, *Nucl. Phys.* **A183**, 60 (1972).

⁸H. Segawa, K. I. Kubo, and A. Arima, *Phys. Rev. Lett.* **35**, 357 (1975).

- ⁹D. K. Olsen, T. Udagawa, T. Tamura, and R. E. Brown, *Phys. Rev. C* **8**, 609 (1973).
- ¹⁰W. S. Chien, C. H. King, J. A. Nolen, and M. A. Shaha-buddin, *Phys. Rev. C* **12**, 332 (1975).
- ¹¹G. Vourvopoulos, M. B. Greenfield, J. B. Ball, S. Raman, and W. K. Dagenhart, *Phys. Lett.* **52B**, 187 (1974).
- ¹²N. B. de Takacsy, *Nucl. Phys.* **A231**, 243 (1974).
- ¹³R. N. Boyd, W. P. Alford, E. R. Flynn, and R. A. Hardekopf, *Phys. Rev. C* **15**, 1160 (1977).
- ¹⁴J. D. Burch, M. J. Schneider, and J. J. Kraushaar, *Nucl. Phys.* **A299**, 117 (1978).
- ¹⁵L. A. Charlton, *Phys. Rev. Lett.* **35**, 1495 (1975).
- ¹⁶V. Managoli, D. Robson, and L. A. Charlton, *Nucl. Phys.* **A290**, 128 (1977).
- ¹⁷K. Yagi, S. Kunori, Y. Aoki, K. Nagano, Y. Toba, and K.-I. Kubo, *Phys. Rev. Lett.* **43**, 1087 (1979).
- ¹⁸S. Kunori, A. Aoki, H. Iida, K. Nagano, Y. Toba, and K. Yagi, *Phys. Rev. Lett.* **46**, 810 (1981).
- ¹⁹R. A. Hardekopf, *Proceedings of the Fourth International Conference on Polarization Phenomena in Nuclear Reactions, Zürich, 1975*, edited by W. Gruebler and V. König (Birkhäuser, Basel, 1976), p. 865.
- ²⁰R. A. Hardekopf, G. G. Ohlsen, R. V. Poore, and N. Jarmie, *Phys. Rev. C* **13**, 2127 (1976).
- ²¹E. R. Flynn, S. Orbesen, J. D. Sherman, J. Sunier, and R. Woods, *Nucl. Instrum. Methods* **128**, 35 (1975).
- ²²P. D. Kunz, code CHUCK, University of Colorado, 1974 (unpublished).
- ²³B. F. Bayman and A. Kallio, *Phys. Rev.* **156**, 1121 (1967).
- ²⁴W. W. True, *Phys. Rev.* **168**, 1388 (1968).
- ²⁵W. W. True, C. W. Ma, and W. T. Pinkston, *Phys. Rev. C* **3**, 2421 (1971).
- ²⁶E. R. Flynn, D. D. Armstrong, J. G. Beery, and A. G. Blair, *Phys. Rev.* **182**, 1113 (1969).
- ²⁷R. A. Hardekopf, L. R. Veaser, and P. W. Keaton, Jr., *Phys. Rev. Lett.* **35**, 1623 (1975).
- ²⁸F. D. Becchetti, Jr. and G. W. Greenlees, *Phys. Rev.* **182**, 1190 (1969).
- ²⁹J. D. Childs, W. W. Daehnick, and M. J. Spisak, *Phys. Rev. C* **10**, 217 (1974).
- ³⁰W. W. Daehnick, J. D. Childs, and Z. Vrcelj, *Phys. Rev. C* **21**, 2253 (1980).
- ³¹R. A. Moyer, B. L. Cohen, and R. C. Diehl, *Phys. Rev. C* **2**, 1898 (1970).
- ³²M. Redlich, *Phys. Rev.* **138**, B544 (1965).
- ³³M. Igarishi and K. I. Kubo, see Ref. 1, p. 715.